

Study on the transformation of surface water and groundwater in the water source area of Baima-Jili River Basin

Zhiwei Qi^{a,b,c}, Ge Wang^{a,b,c} and Bo Zhang^{a,b,c,*}

^a Key Laboratory of Groundwater Resources and Environment, Ministry of Education, Jilin University, No 2519, Jiefang Road, Changchun 130021, China

^b Jilin Provincial Key Laboratory of Water Resources and Environment, Jilin University, No 2519, Jiefang Road, Changchun 130021, China

^c College of New Energy and Environment, Jilin University, No 2519, Jiefang Road, Changchun 130021, China

*Corresponding author. E-mail: jluzhangbo@126.com

ABSTRACT

The exploitation of groundwater in a riverside water source area is a complex process of conversion of surface water and groundwater. At present, the numerical model for simulating the exploitation of riverside water sources often generalizes rivers to the specified head boundary (CHD) or the river boundary (RIV). The CHD generalizes the river into an infinite supply of water, which is obviously unrealistic for seasonal rivers, and the RIV does not have the function of the river confluence. The above two methods directly affect the calculation accuracy of river water and groundwater conversion amount due to inherent loopholes, so the simulation of the riverside exploitation amount has some errors. This study uses the Streamflow-Routing (SFR) model to generalize the Baima-Jili River. By calculating the stream flow, the upstream, and downstream water levels of the rainy, normal, and dry seasons through the permeability parameter between river water and groundwater (parameters such as riverbed permeability coefficient, riverbed thickness, water depth, and cross-sectional shape), a coupling model of surface water and groundwater is established. In order to verify the accuracy of the SFR model simulation, the CHD and RIV conditions are used to generalize the river, and the simulation results of the three models are compared. The results show that the available groundwater exploitation simulated by the SFR model, the CHD, and the RIV boundary conditions are 27.798×10^6 , 35.11×10^6 , and 25.76×10^6 m³/a, respectively. The known available groundwater exploitation in the study area is $2,870 \times 10^4$ m³/a. Therefore, the SFR simulation results are more realistic, indicating that the SFR model is more suitable for coupling simulation of the surface water and groundwater interaction in riverside water sources of a seasonal river.

Key words: river boundary, riverside water source area, specified head boundary, Streamflow-Routing model, surface water and groundwater coupling model

HIGHLIGHTS

- The SFR model is used to profit the river, which is more in line with the actual situation than other profications.
- For river characteristics, better proficiency simulations improve the calculation accuracy.
- SFR simulation is more close to the actual known mining amount, and is more suitable for the simulation of water source in the river.

GRAPHICAL ABSTRACT

ID	HCOND1 (m/d)	THICKM1 (m)	ELEVUP (m)	WIDTH1 (m)	DEPTH1 (m)	HCOND2 (m/d)	THICKM2 (m)	ELEVDN (m)	WIDT (m)
50	0.002	3.0	0.02	100.0	3.0	0.002	3.0	0.015	100.0

1. INTRODUCTION

The aquifers in the riverside water source area usually have the advantages of strong water richness, shallow buried ground-water level, stable water volume, excellent water quality, easy centralized exploitation and management, etc. It is a common type of groundwater exploitation (May & Mazlan 2014; Manoj *et al.* 2019). Affected by multiple factors such as atmospheric precipitation and artificial exploitation, there are close hydraulic connections and complex conversion relationships between river and groundwater (Zhang *et al.* 2019; Zhang & Chui 2020). Especially under the influence of artificial exploitation and other factors, groundwater exploitation actually takes a considerable part of the river water resources. The exploitable amount of groundwater sources near the river is closely related to the stream flow, the permeability of the river bed, the thickness of the aquifer and the water conductivity (Chen & Shu 2002; Shubert 2002; Singh *et al.* 2002). Water intake near the river can stimulate and increase the infiltration recharge of river water to the aquifer (Hantush 1965; Mohaned 2005), so as to realize the joint utilization of surface water and groundwater resources.

Studying the interaction between river and groundwater is of a great significance for understanding regional water cycle patterns and rational development and utilization of water resources. At present, the methods commonly used by scholars mainly include water balance method (Ibrakhimov *et al.* 2018), environmental tracing method, and simulation calculation method. The water balance method (Meng *et al.* 2019) analyzes its rechargeable runoff discharge conditions based on a large amount of statistical data, which are accumulated by many arithmetic formulas, and lack of the physical foundation. Environmental tracing methods usually use isotope tracing information to analyze and calculate the age and source of groundwater and river water (Zhao *et al.* 2018; Wang *et al.* 2019). But for small watersheds where river water and groundwater change quickly, the calculation accuracy is insufficient. Simulation calculation methods include groundwater dynamics model (Osei-Twumasi *et al.* 2016) and river dynamics model (Barati *et al.* 2019). Because of its advantages such as visibility and simulation, it has become a common research method at this stage (Hu *et al.* 2016). In recent years, more and more scholars have devoted themselves to the study of refinement and quantification models. Coupling models between the two have emerged, such as Hydrogeosphere (Gilfedder *et al.* 2019), Inflow (Le Lay *et al.* 2019), and GSflow (Feng *et al.* 2018). Many scholars use coupled simulation method to study the interaction between groundwater and surface water. Jolly *et al.* (2010) pointed out that the interaction between groundwater and surface water in wetlands is affected by factors such as the difference between surface water level and groundwater level, local topography, and groundwater flow field. An *et al.* (2018) established a surrogate-based simulation–optimization approach to identify parameter values for a fully integrated surface water and groundwater flow coupling simulation. A wide variety of approaches to hydrologic modeling of river basins confirms our ability to select models, particularly in the condition of close hydraulic connection. Surfleet *et al.* (2012) compared three structurally distinct approaches and spatial scales of parameterization to establish the catchment hydrology modeling. The characteristic of these coupled models is that groundwater and surface water have mutual boundary conditions, requiring model users to have strong modeling capabilities for both groundwater and surface water. However, their modeling

techniques are difficult and complicated to operate. In contrast, the extended coupling model based on the MODFLOW (Zhang *et al.* 2013), which has been widely used in the groundwater field, will have a wider range of applications.

When establishing a coupling model for surface water and groundwater, most groundwater scholars generalize the river to the specified head boundary (CHD) or RIV (Lautz & Siegel 2006) boundary. These studies simply generalized the river, and did not fully consider the impact of the difference in river level and flow during dry and rainy periods on groundwater exploitation (Zhu *et al.* 2014; Zhang & Liu 2015). However, the connection between surface water and groundwater in this study area is close, and the simple generalization of the river cannot restore the real flow field. In order to make up for the deficiencies of previous studies, this study uses the Streamflow-Routing (SFR) model, the CHD and the RIV boundary conditions to generalize the Baima River-Jili River basin, respectively. Then, by establishing a surface water-groundwater coupling model, the conversion volume of surface water and groundwater and the design exploitation volume of the flow field are obtained. Finally, the simulation results of each model are tested according to the known exploitation volume.

2. STUDY AREA

The Baima-Jili River Basin is located in Jiaonan County, Qingdao City, which belongs to the warm temperate coastal humid monsoon area. The upper part of the basin is wider and the lower part is narrow, and the whole area is fan-shaped. The annual average temperature is 12.5 °C, and the annual average precipitation is 830 mm. The rainy season is from July to September, the normal season is from April to June and October, and the dry season is from November to March. The precipitation in the rainy season can reach more than 60% of the annual precipitation. The river water will dry up during the dry season, and there is a huge difference in flow during rainy and dry water periods. The length of the Jili River and the main stream of the Baima River are 44.2 and 39.85 km, respectively, and the annual average relative humidity is 74%. The study area is located in the middle and lower reaches of Baima River and Jili River, with a total area of about 148.5 km². The north, east, and west of the river are mountains, sandwiching the two river valleys into a 'Y' shape.

According to the genesis, the quaternary loose rock aquifer group of the Baima River can be divided into alluvial sand, gravel layer, slope layer, slope alluvial clay sand with gravel layer, and alluvial-ocean layer. The water-rich groundwater partition is shown in Figure 1. The groundwater replenishment sources are atmospheric precipitation, irrigation infiltration, and river infiltration recharge. After receiving infiltration recharge from atmospheric precipitation in the bedrock area of the study area, groundwater runoff from both sides into the valley and into the valley plain. The direction of groundwater movement is generally consistent with the direction of surface runoff, both moving from upstream to downstream, and the two rivers become the main discharge zone. The discharge modes of groundwater are mainly artificial exploitation, submerged evaporation, and runoff discharge. The seasonal change of groundwater dynamics is obvious, and the dynamic curve is undulating. By the beginning of June, the groundwater level had dropped to the lowest valley, and the water level rebounded rapidly during the high water period from July to September. The main characteristic of inter-annual change is that the water level rises in the year of rainy season and the water level decreases in the year of dry season.

3. RESEARCH METHOD

The SFR model is a river bed confluence model designed by US Geological Survey (Prudic *et al.* 2004). The principle is the diffusion wave equation omitting the acceleration term. The source of water intake in the middle and lower reaches of the Baima-Jili River Basin is mainly groundwater and supplemented by surface water. In order to better plan the rational development and utilization of water resources in this area, this study comprehensively considers the interaction between the channel flow of the Baima-Jili River and the saturated zone of the aquifer. Connected with the permeability between the river water and groundwater (parameters such as riverbed permeability coefficient, riverbed thickness, water depth, and cross-sectional shape), then, SFR and MODFLOW are automatically coupled to calculate the stream flow and the upstream and downstream water levels during the rainy, normal, and dry seasons. The generalization of the river is more in line with the actual situation of the Baima-Jili River Basin. The calculation of the conversion amount between the river and the aquifer is more accurate, and the calculation accuracy of groundwater resources in the water source is improved. Then, the Baima-Jili River was generalized into the CHD and the RIV boundary conditions, and the groundwater exploitability in the three-river generalized condition was trial-calculated. In the end, a comparative analysis was carried out based on the maximum groundwater exploitation obtained from actual surveys.

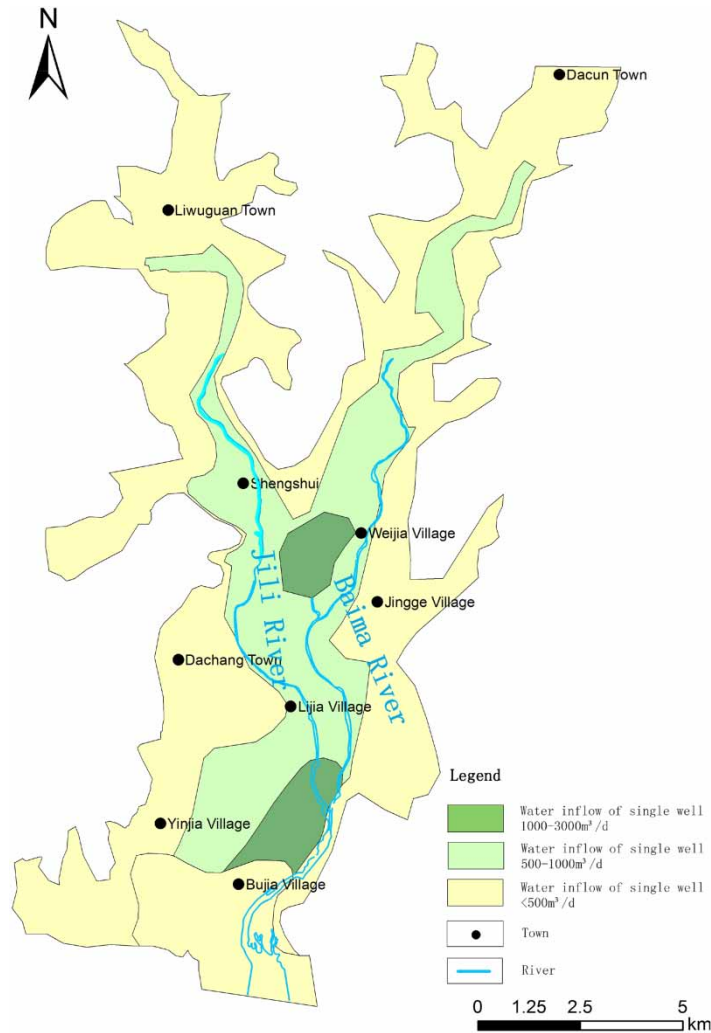


Figure 1 | Subsurface water-rich zoning.

3.1. Groundwater numerical model

The corresponding mathematical model is established according to the hydrogeological conceptual model as follows:

$$\begin{cases} \frac{\partial}{\partial x} (k_x \frac{\partial h}{\partial x}) + \frac{\partial}{\partial y} (k_y \frac{\partial h}{\partial y}) + \frac{\partial}{\partial z} (k_z \frac{\partial h}{\partial z}) - W = \mu \frac{\partial h}{\partial t} \\ h(x, y, z, t)|_{\Sigma_1} = h_1(x, y, z) \quad x, y, z \in \Sigma_1 \\ h(x, y, z, 0) = h_0(x, y, z) \quad x, y, z \in D \end{cases} \quad (1)$$

where h is the groundwater head (m), K_x , K_y , K_z are the x , y , z direction permeability coefficient respectively (m/d), h_1 is the aquifer first boundary head (m), h_0 is the aquifer initial head (m), W is the intensity of source and sink items (including exploitation intensity, etc.) (m^3/d), Σ_1 is the first boundary of aquifer, D represents the research area, μ is the water supply coefficient.

3.2. The establishment of SFR mathematical model

The SFR model is established based on the hydrological data of the Baima-Jili River Basin. On the one hand, the river bed receives replenishment from surface confluence, and on the other hand, flow exchange occurs with the underground aquifer. The confluence relationship between the river bed and the underground aquifer is also expressed in the source-sink term. In this way, the source-sink term is divided into two parts: q_s surface confluence and q_u underground confluence. At the same

time, in order to simplify the calculation, the motion equation omits the accelerated motion of the river water, and the Manning formula is used to describe the motion of the river water. So, Saint-Venant's equations were rewritten as:

$$\begin{cases} B \frac{\partial h}{\partial t} + \frac{\partial Q}{\partial x} = q_s + q_u \\ \frac{\partial h}{\partial x} = S_0 - S_f \end{cases} \quad (2)$$

where B is the water surface width (m); q_s is the surface confluence (m^3/d); q_u is the underground confluence (m^3/d); S_0 means the river bed slope; S_f means the friction drop.

The boundary condition of the source-sink term of the equation is the flow process of the initial unit of the river. The q_s and q_u are calculated from surface rainfall overflow and underground confluence, respectively. In this way, it can be analyzed that the boundary conditions of the differential equation of groundwater flow are the water level and discharge provided by the river diffusion wave equation, and the source-sink terms of the river diffusion equation are calculated by the differential equation of groundwater flow.

3.3. Exchange mechanism and coupling model

Exchange flow is divided into three modes, one is that the groundwater level is higher than the river bed, and the other is that the groundwater level is slightly lower than the river bed. Both of these are saturated seepage mechanisms. The vertical and lateral seepage of the river channel are functions of the difference between the groundwater and the river water head. The third is that the groundwater level is much lower than the riverbed, and unsaturated seepage is formed between them. Regardless of the above modes, the water level difference between the river channel and the aquifer determines the exchange volume between themselves. The coupling model is solved coupling with the river matrix and the groundwater matrix for each time step, thus improving the performance of interactive calculation. The numerical equation of groundwater flow and the diffusion wave equation simultaneously is solved to obtain q_u . The permeability of the river bed is calculated by the following formula:

$$C = \frac{k}{L} \frac{Lw}{t} = \frac{k}{t} w \quad (3)$$

where C is the bed hydraulic conductivity coefficient; k is the bed permeability coefficient (m/d); w is the bed width (m); t is the bed thickness (m); L is the upstream and downstream distance (m).

3.4. Statistical data

The data used in the model include: (1) flow monitoring and precipitation data in the current year of 2017 (Figure 2); (2) 25 groundwater levels measured in the current year of 2017, distributed from the south to the north of the study area, and

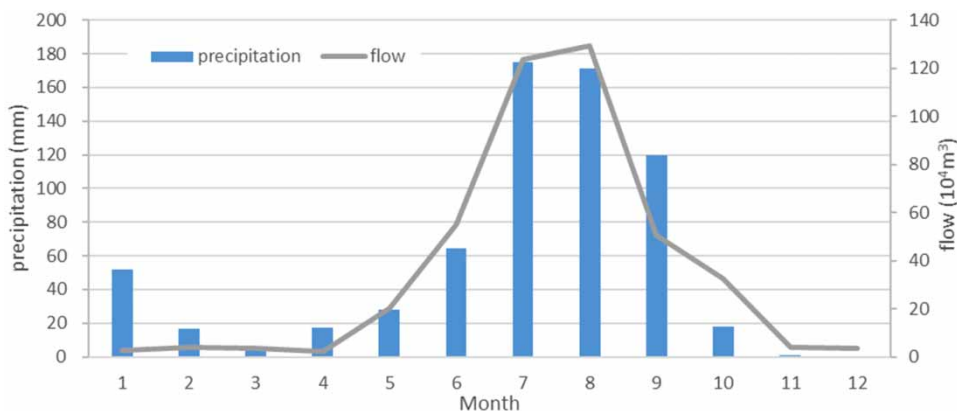


Figure 2 | Annual cumulative monthly rainfall discharge hydrograph.

the flow monitoring points are located in the middle reaches (Figure 3); and (3) the upstream and downstream riverbed shape is generalized as trapezoid, as shown in Figure 4.

4. RESULTS

4.1. Hydrogeological conceptual model

According to the analysis of basic hydrogeological conditions and hydrodynamic field, the conceptual model is determined.

- **Aquifer generalization:** the stratum is generalized into three layers: The first layer is fine sand layer with slightly weak permeability, the second layer is coarse sand gravel layer with strong water permeability, and the third layer is bedrock (as shown in Figure 5).
- **Generalization of hydrodynamic conditions:** The study area is generalized as heterogeneous and isotropic water bearing system, groundwater movement conforms to Darcy's law, groundwater flow can be generalized into three-dimensional Darcy flow when water level changes with time.
- **Generalization of boundary conditions:** The lower reaches of Baima River and Jili River are connected to the sea outlet, which is set as the boundary of constant water head. The water level of the outlet is stable all the year round, and the elevation is 0, which is generalized as a class of head boundary. There are mountains in the east, west, and north of the valley, and the groundwater ridge on three sides is generalized as zero-flow boundary.

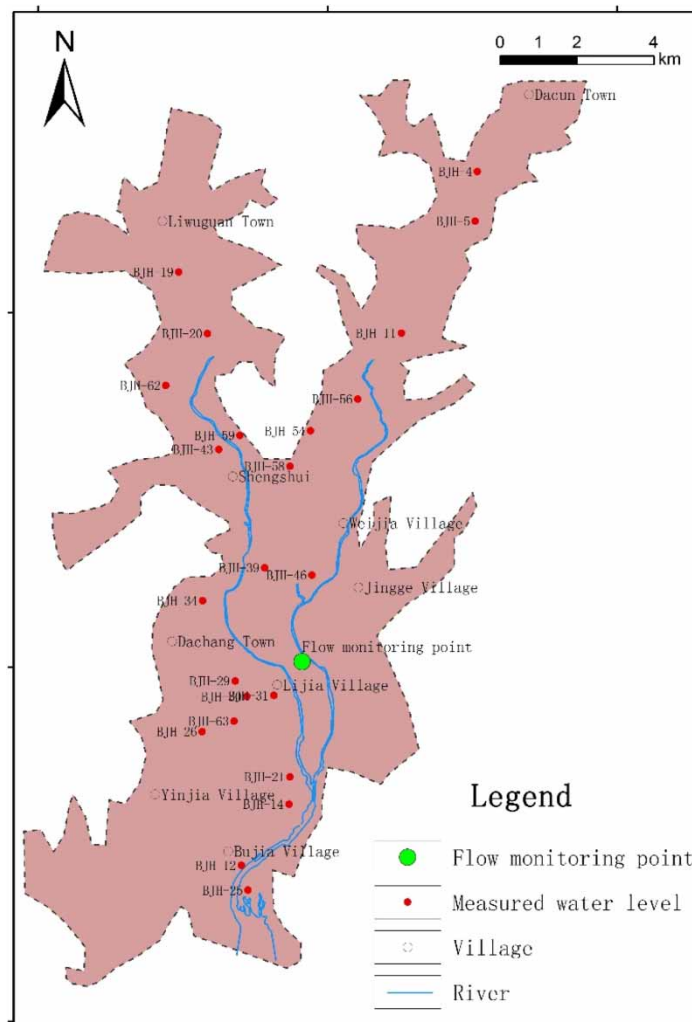


Figure 3 | Distribution of measured well points and flow monitoring points.

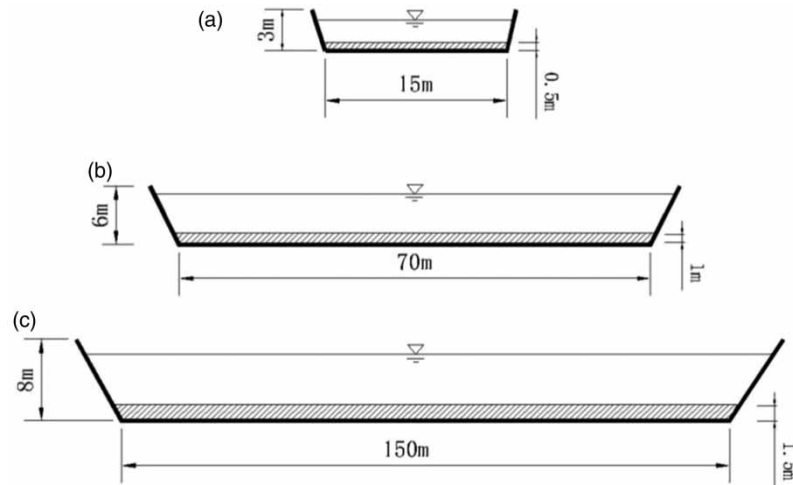


Figure 4 | River channel shape generalization: (a) upstream channel, (b) midstream channel, and (c) downstream channel.

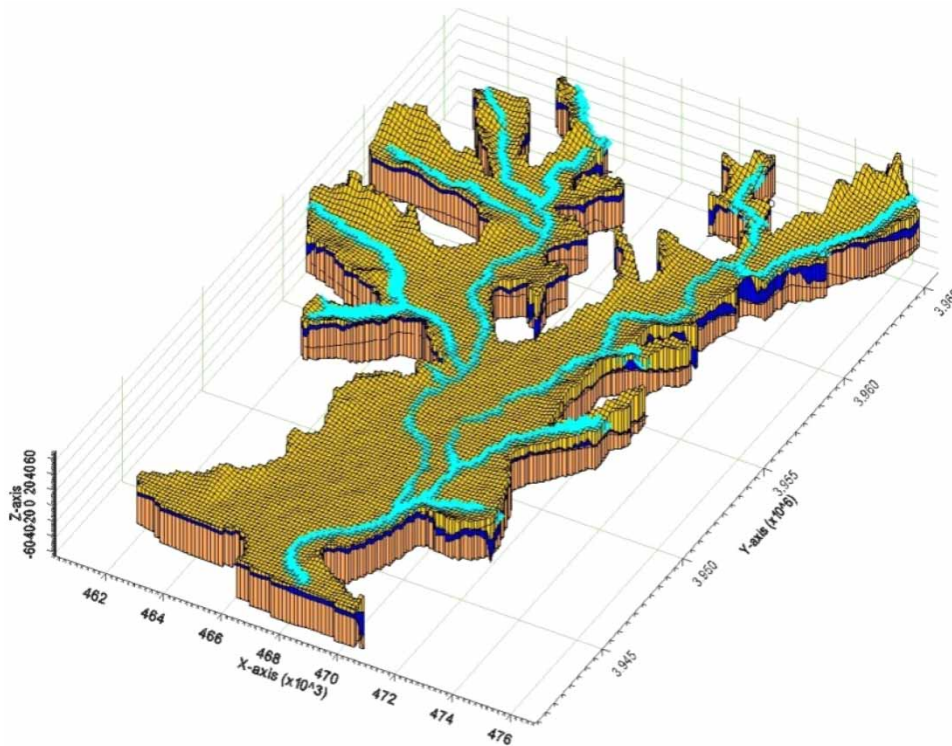


Figure 5 | Model generalization of the study area.

- The generalization of source and sink terms: The precipitation and irrigation infiltration coefficient are treated as surface infiltration; the evaporation is calculated by setting the evaporation limit depth and evaporation rate by ET module; the water source exploitation and discharge are treated by point and area discharge.
- Generalization of boundary conditions: The river boundary is generalized as SFR, the CHD and the RIV boundary conditions, respectively.

The parameters involved in the model mainly include precipitation recharge coefficient, irrigation recharge coefficient, exploitation coefficient, and evaporation coefficient. The precipitation infiltration recharge coefficient is

5.2×10^{-4} – 1.178×10^{-3} m/d in the study area, and the irrigation infiltration recharge coefficient is 2.4×10^{-4} m/d in the irrigated area and 0 m/d in the non-irrigated area, the exploitation coefficient is set to 6×10^{-4} m/d; the evaporation is considered as uniform surface evaporation, and the evaporation coefficient in the partition is set to 1×10^{-4} m/d; the model has three layers, the vertical permeability coefficient of each layer, the horizontal permeability coefficient, water supply, and water storage coefficient are given in the model according to the actual investigation and data collection.

4.2. Conceptual model of river dynamics

According to the field survey, the riverbed in the upper, middle and lower reaches is generalized as trapezoidal riverbed with variable width. The riverbed shape and slope are given by the actual survey. The Baima-Jili River is generalized as SFR, and the slope runoff is set according to rainfall. According to the exploration, the riverbed permeability coefficient, riverbed thickness, cross-sectional shape, and other parameters are set to make the river generalization more in line with the actual situation of the Baima-Jili River. The water level and discharge of each river section are automatically calculated by the SFR model. In addition, the river is generalized as the CHD and the RIV boundary conditions. This simulation mainly verifies the difference between the conversion of river water and groundwater and the amount of available groundwater exploitation under three different boundary conditions of rivers. Thus, to determine the advantages and disadvantages of the three methods. River bed parameters head-stage is set to 8 m. In the SFR model, the flow is input with variable flow, and the remaining parameters are shown in Figure 6. Parameters such as the shape of the river bed are provided by the model.

4.3. Model identification and verification

The groundwater level line measured in this study area during the dry season was identified and compared with the actual water level line in the dry season through the numerical model simulation. Two periods of the current year (January to March and July to September in 2017) are selected to identify and verify the model (Figures 7 and 8). The fitting errors between the calculated water level and the measured water level in the model identification period were statistically analyzed. It shows that the nodes with water level fitting error less than 0.5 m accounted for more than 75% of the number of nodes with known water level. The comparison between the measured value and the simulated value of the observation well in the wet season and the dry season is shown in the following figures (Figures 9 and 10). During the model verification period, the flow field in the rainy season is very close to the measured flow field. The model verification shows that the simulation has high accuracy and credibility.

4.4. Production capacity setting of well points near the river

Exploited wells are set up along the river to simulate real exploitation scenarios, as shown in Figure 11. The exploited wells are mainly arranged along the sides of the river, totaling 130.

The current groundwater level in this study area has dropped to two-thirds of the aquifer thickness. Therefore, when the groundwater level calculated by the model drops by two-thirds of the aquifer thickness, it is the allowable amount of groundwater to be exploited. For the three models of SFR, RIV, and CHD, exploited wells are set-up at the same location,

ID	HCOND1 (m/d)	THICKM1 (m)	ELEVUP (m)	WIDTH1 (m)	DEPTH1 (m)	HCOND2 (m/d)	THICKM2 (m)	ELEVDN (m)	WIDT (m)
50	0.002	3.0	0.02	100.0	3.0	0.002	3.0	0.015	100.0

Figure 6 | SFR model parameter settings.

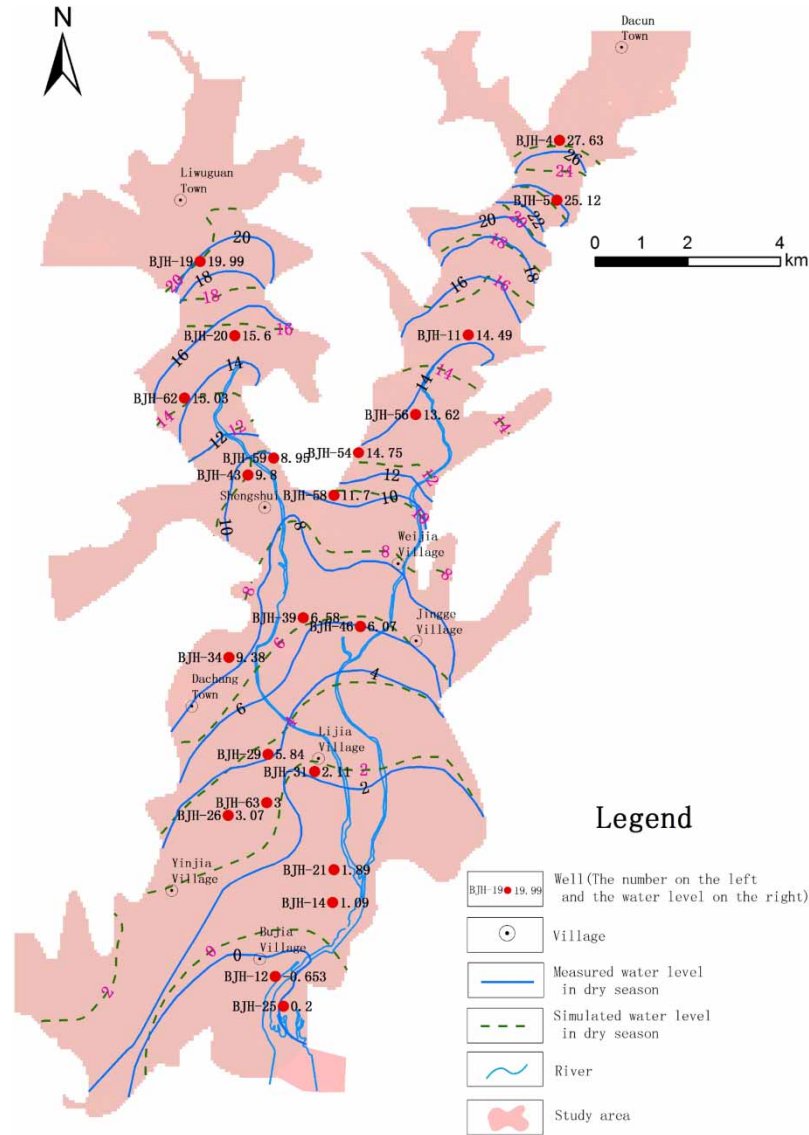


Figure 7 | Measured water level and calculated flow field during the model identification period.

respectively. Exploitable amount of the well points is calculated and the maximum allowable groundwater exploitation volume is compared when the groundwater level drops by two-thirds of the thickness of the aquifer.

Through trial calculation, the main exploitation ability of each well in the rainy, normal, and dry seasons is 700–900 m³/d, and that of RIV boundary conditions well is 700–800 m³/d. However, the calculated exploitation volume under CHD conditions is larger than the former, and the annual exploitation volume per well ranges from 900 to 1,000 m³/d.

5. DISCUSSION

In this simulation, SFR is used to generalize Baimajili River Basin, and the coupling model of surface water and groundwater is established. Compared with the traditional groundwater numerical model, it takes into account the influence of river discharge variation on groundwater exploitation in rainy and dry seasons. The recharge of river water to groundwater should not be ignored. When exploiting groundwater near river when only using the traditional groundwater numerical model to evaluate the exploitation of groundwater near the river, there may be some deviation. In order to verify the rationality of the method proposed in this study, the CHD and RIV boundary conditions are also used to establish the numerical model of groundwater exploitation near the river, and the evaluation conclusion of SFR model is compared. The result of water balance is shown in Table 1.

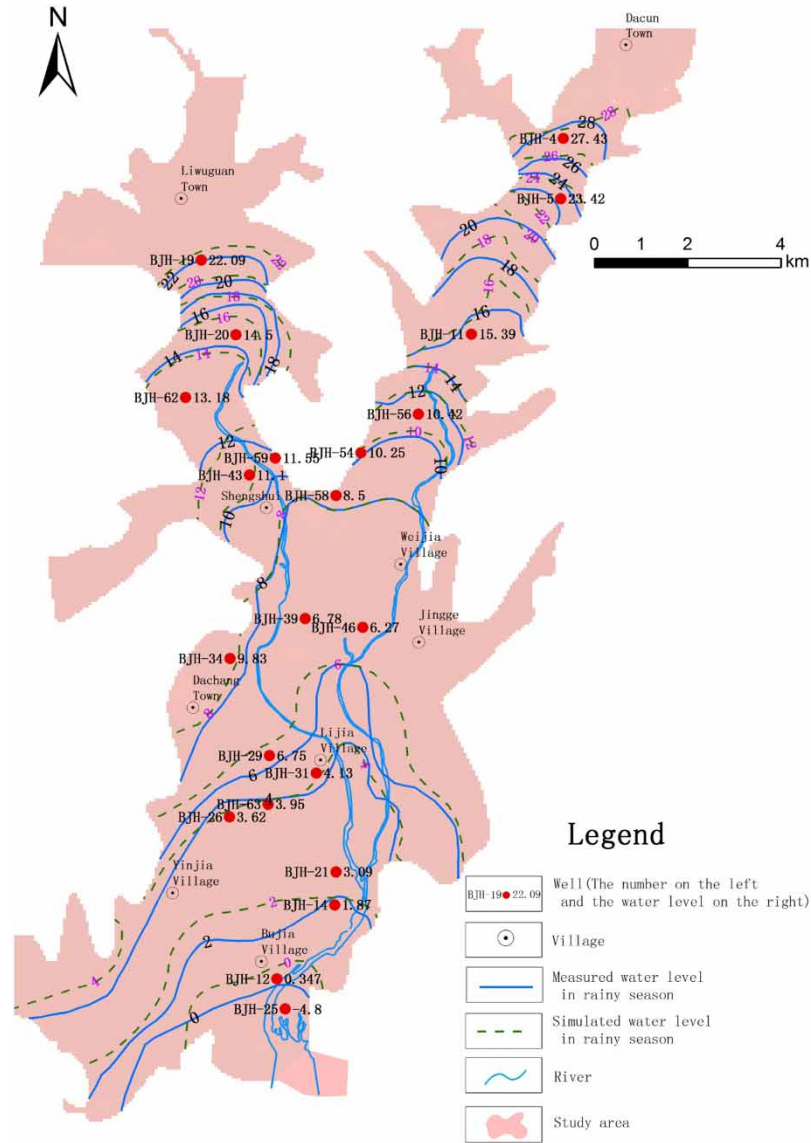


Figure 8 | Measured water level and calculated flow field during the model validation period.

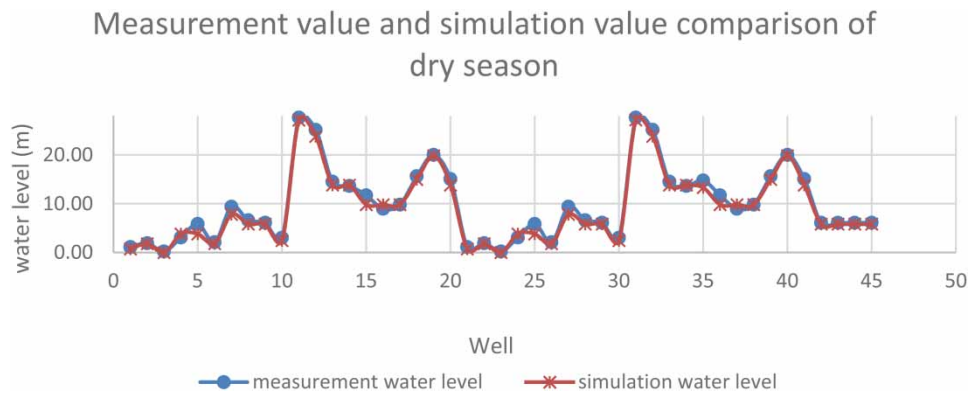


Figure 9 | Measured water and simulation value comparison of dry season.

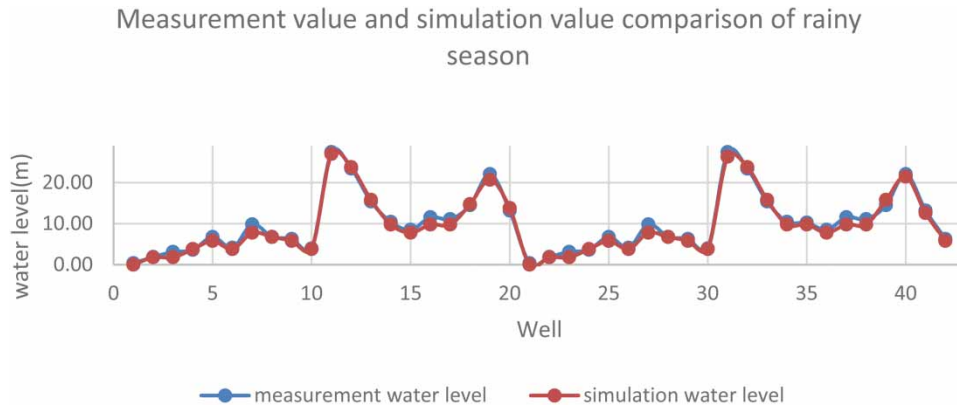


Figure 10 | Measured water and simulation value comparison of rainy season.

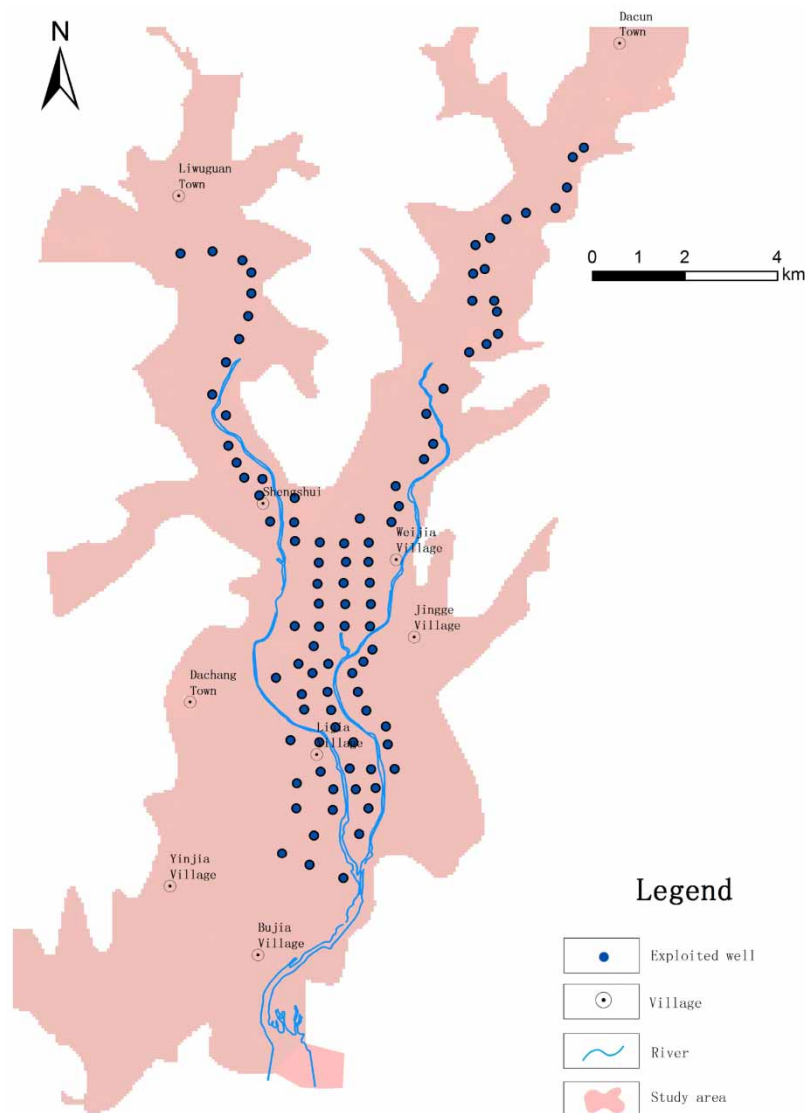


Figure 11 | Simulated exploited well location.

Table 1 | Water balance table (unit: $10^4 \text{ m}^3/\text{d}$)

Period	Module	River feeding	Rainfall infiltration	Seawater supply	Increase in reserves	Total supply	Drain to the river	Well exploitation	Evaporation	Drain into seawater	Drainage ditch	Reduced reserves	Total excretion	Difference between the supply and excretion
Rainy season	SFR	3.08	11.3	0.39	6.01	20.79	2.66	8.39	8.97	0.04	0.4	0.33	20.79	0.0032
	RIV	2.83	11.41	0.57	5.11	19.91	5.73	7.4	6.53	0.02	0.21	0.03	19.92	-0.0003
	CHD	7.55	11.48	0.21	5.56	24.8	5.67	10.82	7.37	0.05	0.15	0.73	24.8	0.0004
Normal season	SFR	2.39	9.98	0.4	4.19	16.96	2.3	7.4	6.95	0.04	0.16	0.11	16.96	-0.0055
	RIV	1.77	9.93	0.57	3.38	15.66	3.57	7	4.98	0.02	0.07	0.02	15.65	0.0034
	CHD	9.46	9.44	0.22	3.25	22.36	5.78	9.24	7.15	0.05	0.05	0.08	22.35	0.0124
Dry season	SFR	2.27	9.68	0.4	3.37	15.72	2.4	7.05	5.77	0.04	0.15	0.3	15.72	-0.0001
	RIV	1.42	9.38	0.57	2.91	14.28	2.85	6.77	4.54	0.02	0.06	0.05	14.28	-0.0048
	CHD	9.99	8.98	0.22	1.48	20.67	4.72	8.8	6.93	0.05	0.04	0.13	20.68	-0.007

5.1. Comparative analysis of SFR and CHD models

5.1.1. Comparing the conversion of surface water and groundwater

Comparing the river recharge and discharge volume of SFR model and CHD conditions, it can be seen from Table 1 that the groundwater recharge quantity of SFR model and CHD conditions are 3.08×10^4 and 7.55×10^4 m³/d, respectively, in rainy season. In normal season, the groundwater recharge quantity of the SFR model and CHD conditions are 2.39×10^4 and 9.46×10^4 m³/d, respectively, and river discharge are 2.3×10^4 and 5.78×10^4 m³/d. In the dry season, the groundwater recharge quantity of SFR model and CHD conditions are 2.27×10^4 and 9.99×10^4 m³/d, respectively, and the amount of groundwater converts to the river water are 2.4×10^4 and 4.72×10^4 m³/d.

Compared with the two models in the rainy, normal, and dry seasons in Figure 12, the recharge amount to river water of specified head boundary is the largest. Especially in the dry season when there is little precipitation, the river water will recharge the groundwater more. During the rainy, normal, and dry seasons, the amount of groundwater supplied by the river is greater than the discharge amount of groundwater to the river, that is, the river has always supplied to the groundwater.

In contrast, the conversion of river water to groundwater is relatively balanced in the SFR model. River recharge is greater than river discharge in rainy season, and river recharge and river discharge are basically the same in normal water period, while river recharge is less than river discharge in dry season. This is a typical recharge mode of the groundwater replenishing the surface water. Under CHD conditions, the river water recharges more to the groundwater in the dry season, which proves the irrationality of the specified head boundary. Because it is ‘the boundary of unlimited water supply’, which is obviously inconsistent with the seasonal river such as the Baima river and Jili river. To sum up, the SFR model can calculate the conversion between surface water and groundwater more accurately than the CHD conditions, and the calculation results are reasonable.

5.1.2. Comparison of simulation exploitation volume

It can be seen from Table 1 that the exploitable quantities calculated by the SFR model and CHD conditions are 8.39×10^4 and 10.82×10^4 m³/d, respectively, in rainy season; and that by the SFR model and CHD conditions in normal season are 7.4×10^4 and 9.24×10^4 m³/d. In dry season, the exploitable quantities calculated by the SFR model and CHD conditions are 7.05×10^4 and 8.8×10^4 m³/d, respectively.

As shown in Figure 13 that the simulated exploitation amount under CHD conditions is larger than the SFR in each period. The maximum allowable exploitation amount simulated by the CHD is 35.11 million m³/a, which is larger than the known exploitable groundwater amount of 28.7 million m³/a in the study area. While the simulated exploitation amount of SFR is 27.79 million m³/a. The simulation result of SFR model is more in line with the reality than that of the CHD conditions, and the planned exploitation amount of the exploited wells is more reasonable.

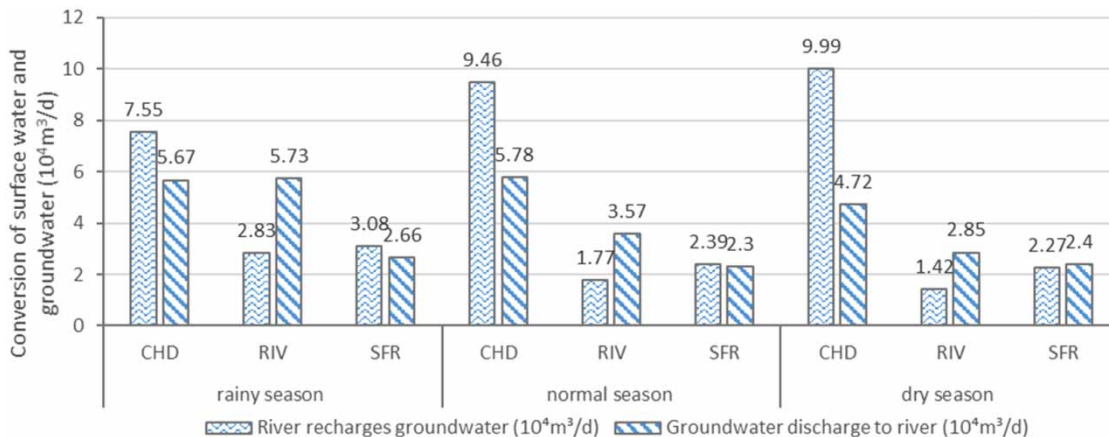


Figure 12 | Transformation of surface water and groundwater in different periods.

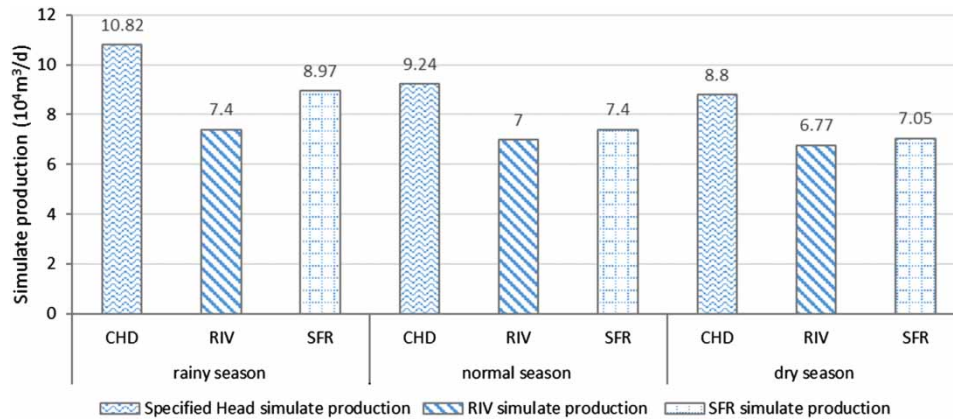


Figure 13 | Simulated production in different periods.

5.2. Comparative analysis of SFR and RIV models

The RIV boundary is also the traditional boundary condition of the MODFLOW. It generalizes the river by setting parameters such as upstream and downstream river water level, riverbed elevation, and hydraulic conductivity coefficient. The common point of the boundary between RIV and SFR is that the hydraulic exchange between groundwater and river water is realized through the permeability parameters of the river. However, RIV boundary does not have the function of confluence, and its water level and width are set by the user. So, RIV boundary condition requires a large amount of long-term observation data and is not as flexible as the SFR model.

5.2.1. Comparing the conversion of surface water and groundwater

As shown in Table 1, the groundwater recharge quantity by the SFR model and RIV condition are 3.08×10^4 and 2.83×10^4 m³/d, respectively, in rainy season. The amount of river water replenishing groundwater by the SFR model and RIV condition are 2.39×10^4 and 1.77×10^4 m³/d in normal season, and the river discharge are 2.3×10^4 and 3.57×10^4 m³/d, respectively. In the dry season, the groundwater recharge quantity by SFR model and RIV condition are 2.27×10^4 and 1.42×10^4 m³/d, respectively, and the groundwater discharged from river are 2.4×10^4 and 2.85×10^4 m³/d.

It can be seen from the comparison between the two models in the rainy, normal, and dry seasons in Figure 12 that the discharge mode under the RIV boundary condition is the groundwater that continuously recharges to the river water, whereas the drainage mode of the SFR model is not unique. Comparing SFR and RIV model's recharge and discharge quantity in different periods, it can be seen that the SFR model has a more balanced relationship between surface water and groundwater conversion. The recharge amount of river water to groundwater in each period under the RIV boundary condition is similar to the result of SFR, while the amount of groundwater discharged to the river under the RIV boundary condition is larger. It is because the SFR model has a confluence function. However, the RIV boundary can only input the water level by the user, and calculate the conversion between the river water and the groundwater through the water level difference between them. In fact, the river water resources were taken away due to the massive exploitation of groundwater during the dry season. The river has been cut off, and the groundwater has long been unable to recharge the river. Therefore, the amount of groundwater recharge to the river in RIV boundary simulation is larger. The SFR model simulation results are more consistent with the conversion relationship between surface water and groundwater in the study area during the rainy, normal, and dry seasons.

5.2.2. Comparison of simulation exploitation volume

It can be seen from Table 1 that the exploitable quantities calculated by the SFR model and RIV boundary condition in rainy season are 8.39×10^4 and 7.4×10^4 m³/d, respectively. In normal season, the exploitable quantities calculated by the SFR model and RIV boundary condition are 7.4×10^4 and 7×10^4 m³/d, whereas in dry season are 7.05×10^4 and 6.77×10^4 m³/d, respectively.

According to Figure 13, the simulated exploitation amount of SFR model is slightly larger than that of the RIV condition in the rainy, normal, and dry season. The known exploitable amount of groundwater in this study area is 28.7 million m³/a, and that of the SFR model is 27.79 million m³/a. The simulated exploitation amount under the RIV condition is

25.76 million m³/a, which is less than the maximum allowable exploitation amount. Therefore, compared with RIV condition, the SFR simulation results are more realistic and the simulated exploitation volume is more reasonable.

6. CONCLUSION

The exploitation of riverside water sources usually involves complex situations of conversion between surface water and groundwater. This study comprehensively considers the stream flow difference of the Baima-Jili River during rainy and dry seasons, using SFR, CHD, and RIV boundary conditions to simulate the conversion of river water and surface water. The results showed that when a part of the river was cut off, the river water no longer supplied the groundwater for exploitation. Although the boundary of the CHD is unlimitedly replenished, the calculated resource amount is significantly larger than the actual survey data. The RIV boundary needs to be based on a large number of river water level station observation data, and the water level of each river section is artificially given, which is not suitable for widespread use. However, the SFR model can automatically calculate the stream flow and water level of each river section, which better solves the problems of the specified head boundary and RIV boundary. The SFR model couples the river model with the groundwater model, so that the river generalization is more in line with the actual conditions of the Baima-Jili River Basin, and the conversion of surface water and groundwater is calculated more accurately. In the example of this article, the exploitation volume simulated by SFR is closer to the known exploitation volume of groundwater in this study area. In summary, the surface water and groundwater coupling model of SFR is more suitable than the traditional groundwater numerical model for calculating the conversion volume of surface water and groundwater and evaluating the extraction volume of groundwater in the riverside water source area.

CONFLICT OF INTEREST

None.

DATA AVAILABILITY STATEMENT

All relevant data are included in the paper or its Supplementary Information.

REFERENCES

- An, Y. K., Lu, W. X. & Yan, X. M. 2018 A surrogate-based simulation-optimization approach application to parameters' identification for the HydroGeoSphere model. *Environmental Earth Sciences* **77**, 621. <https://doi.org/10.1007/s12665-018-7806-7>.
- Barati, A. A., Azadi, H. & Scheffran, J. 2019 A system dynamics model of smart groundwater governance. *Agricultural Water Management* **221**, 502–518. <https://doi.org/10.1016/j.agwat.2019.03.047>.
- Chen, X. H. & Shu, L. C. 2002 Stream-aquifer interactions: evaluation of depletion volume and residual effects from ground water pumping. *Ground Water* **40**, 284–290. <https://doi.org/10.1111/j.1745-6584.2002.tb02656.x>.
- Feng, D. P., Zheng, Y., Mao, Y. X., Zhang, A. J., Wu, B., Li, J. G., Tian, Y. & Wu, X. 2018 An integrated hydrological modeling approach for detection and attribution of climatic and human impacts on coastal water resources. *Journal of Hydrology* **557**, 305–320. <https://doi.org/10.1016/j.jhydrol.2017.12.041>.
- Gilfedder, B. S., Cartwright, I., Hofmann, H. & Frei, S. 2019 Explicit modeling of Radon-222 in HydroGeoSphere during steady state and dynamic transient storage. *Groundwater* **57**, 36–47. <https://doi.org/10.1111/gwat.12847>.
- Hantush, M. S. 1965 Well near streams with semipervious beds. *Journal of Geophysical Research* **12**, 2829–2838.
- Hu, L. T., Xu, Z. X. & Huang, W. D. 2016 Development of a river-groundwater interaction model and its application to a catchment in Northwestern China. *Journal of Hydrology* **543**, 483–500. <https://doi.org/10.1016/j.jhydrol.2016.10.028>.
- Ibrakhimov, M., Awan, U. K., George, B. & Liaqat, U. W. 2018 Understanding surface water-groundwater interactions for managing large irrigation schemes in the multi-country Fergana valley, Central Asia. *Agricultural Water Management* **201**, 99–106. <https://doi.org/10.1016/j.agwat.2018.01.016>.
- Jolly, I. D., McEwan, K. L. & Holland, K. L. 2010 A review of groundwater-surface water interactions in arid/semi-arid wetlands and the consequences of salinity for wetland ecology. *Ecohydrology* **1**, 43–58. <https://doi.org/10.1002/eco.6>.
- Lautz, L. K. & Siegel, D. I. 2006 Modeling surface and ground water mixing in the hyporheic zone using MODFLOW and MT3D. *Advances in Water Resources* **29**, 1618–1633. <https://doi.org/10.1016/j.advwatres.2005.12.003>.
- Le Lay, H., Thomas, Z., Rouault, F., Pichelin, P. & Moatar, F. 2019 Characterization of diffuse groundwater inflows into stream water (Part II: quantifying groundwater inflows by coupling FO-DTS and vertical flow velocities). *Water* **11**, 2430. <https://doi.org/10.3390/w11122430>.
- Manoj, S., Thirumurugan, M. & Elango, L. 2019 Hydrogeochemical modelling to understand the surface water-groundwater interaction around a proposed uranium exploitation site. *Journal of Earth System Science* **128**, 49. <https://doi.org/10.1007/s12040-019-1078-9>.

- May, R. & Mazlan, N. S. B. 2014 Numerical simulation of the effect of heavy groundwater abstraction on groundwater–surface water interaction in Langat Basin, Selangor, Malaysia. *Environmental Earth Sciences* **71**, 1239–1248. <https://doi.org/10.1007/s12665-013-2527-4>.
- Meng, F. A., Xiao, C. L., Liang, X. J., Wang, G. & Sun, Y. 2019 Regularity and a statistical model of surface water and groundwater interaction in the Taoer River alluvial fan, China. *Water Science and Technology-Water Supply* **19**, 2379–2390. <https://doi.org/10.2166/ws.2019.118>.
- Mohaned, M. H. 2005 Modeling stream-aquifer interactions with linear response functions. *Journal of Hydrology* **311**, 59–79. <https://doi.org/10.1016/j.jhydrol.2005.01.007>.
- Osei-Twumasi, A., Falconer, R. A. & Ahmadian, R. 2016 Coupling surface water and groundwater flows in a laboratory model using foam as artificial groundwater material. *Water Resources Management* **30**, 1449–1463. <https://doi.org/10.1007/s11269-016-1232-y>.
- Prudic, D. E., Konikow, L. F. & Banta, E. R. 2004 *A new Streamflow-Routing (SFR1) Package to Simulate Stream-aquifer Interaction with MODFLOW-2000*. U.S. Geological Survey, Reston, VA. Open-File Report, pp. 2004–1042.
- Shubert, J. 2002 Hydraulic aspects of riverbank filtration – field studies. *Journal of Hydrology* **266**, 145–161. [https://doi.org/10.1016/S0022-1694\(02\)00159-2](https://doi.org/10.1016/S0022-1694(02)00159-2).
- Singh, S. K., Mishra, G. C., Swamee, P. K. & Ojha, C. S. P. 2002 Aquifer diffusivity and stream resistance from varying stream stage. *Journal of Irrigation and Drainage Engineering* **128**, 57–61. [https://doi.org/10.1061/\(ASCE\)0733-9437\(2002\)128:1\(57\)](https://doi.org/10.1061/(ASCE)0733-9437(2002)128:1(57)).
- Surfleet, C. G., Tullios, D., Chang, H. & Jung, I. W. 2012 Selection of hydrologic modeling approaches for climate change assessment: a comparison of model scale and structures. *Journal of Hydrology* **464**, 233–248. <https://doi.org/10.1016/j.jhydrol.2012.07.012>.
- Wang, Y., Dong, R., Zhou, Y. Z. & Luo, X. 2019 Characteristics of groundwater discharge to river and related heavy metal transportation in a mountain exploitation area of Dabaoshan, Southern China. *Science of The Total Environment* **679**, 346–358. <https://doi.org/10.1016/j.scitotenv.2019.04.273>.
- Zhang, K. & Chui, T. F. M. 2020 Assessing the impact of spatial allocation of bioretention cells on shallow groundwater – an integrated surface-subsurface catchment-scale analysis with SWMM-MODFLOW. *Journal of Hydrology* **586**, 124910. <https://doi.org/10.1016/j.jhydrol.2020.124910>.
- Zhang, A. J. & Liu, J. 2015 Exploring scale dependent ecohydrological responses in a large endorheic river basin through integrated surface water groundwater modeling. *Water Resources Research* **51**, 4065–4085. <https://doi.org/10.1002/2015WR016881>.
- Zhang, B., Hong, M., Zou, Z. H., Jim, Y. T. & Cheng, P. 2013 Embedding isochronous cells overland flow module into MODFLOW. *Hydrological Processes* **27**, 3833–3841. <https://doi.org/10.1002/hyp.9475>.
- Zhang, J., Wang, W. K., Wang, X. Y., Yin, L. H., Zhu, L. F., Sun, F. Q., Dong, J. Q., Xie, Y. Q., Robinson, N. I. & Love, A. J. 2019 Seasonal variation in the precipitation recharge coefficient for the Ordos Plateau, Northwest China. *Hydrogeology Journal* **27**, 801–813. <https://doi.org/10.1007/s10040-018-1891-2>.
- Zhao, D., Wang, G. C., Liao, F., Yang, N., Jiang, W. J., Guo, L., Liu, C. L. & Shi, Z. M. 2018 Groundwater–surface water interactions derived by hydrochemical and isotopic (^{222}Rn , deuterium, oxygen-18) tracers in the Nomhon area, Qaidam Basin, NW China. *Journal of Hydrology* **565**, 650–661. <https://doi.org/10.1016/j.jhydrol.2018.08.066>.
- Zhu, F. F., Huang, W. R., Cai, Y., Teng, F., Wang, B. B. & Zhou, Q. 2014 Development of a river hydrodynamic model for studying surface-ground water interactions affected by climate change in Heihe River, China. *Journal of Coastal Research* **S.68**, 129–135. <https://doi.org/10.2112/SI68-017.1>.

First received 17 January 2022; accepted in revised form 18 March 2022. Available online 13 April 2022